JACS
JOURNAL OF THE AMERICAN CHEMICAL SOCIETY
Article
pubs.acs.org/JACS

Anticancer β-Hairpin Peptides: Membrane-Induced Folding Triggers Activity

Chomdao Sinthuvanich,[†,‡,Δ] Ana Salomé Veiga,[†,§,Δ] Kshitij Gupta,[⊥] Diana Gaspar,[§] Robert Blumenthal,[⊥] and Joel P. Schneider*[,†]

[†]Chemical Biology Laboratory, National Cancer Institute, Frederick, Maryland 21702, United States

[‡]Department of Chemistry and Biochemistry, University of Delaware, Newark, Delaware 19716, United States

[§]Instituto de Medicina Molecular, Faculdade de Medicina da Universidade de Lisboa, Av. Prof. Egas Moniz, 1649-028 Lisbon, Portugal

[⊥]Membrane Structure and Function Section, Nanobiology Program, National Cancer Institute Frederick, Maryland 21702, United States

Supporting Information

ABSTRACT: Several cationic antimicrobial peptides (AMPs) have recently been shown to display anticancer activity via a mechanism that usually entails the disruption of cancer cell membranes. In this work, we designed an 18-residue anticancer peptide, SVS-1, whose mechanism of action is designed to take advantage of the aberrant lipid composition presented on the outer leaflet of cancer cell membranes, which makes the surface of these cells electronegative relative to the surface of noncancerous cells. SVS-1 is designed to remain unfolded and inactive in aqueous solution but to preferentially fold at the surface of cancer cells, adopting an amphiphilic β-hairpin structure capable of membrane disruption. Membrane-induced folding is driven by electrostatic interaction between the peptide and the negatively charged membrane surface of cancer cells. SVS-1 is active against a variety of cancer cell lines such as A549 (lung carcinoma), KB (epidermal carcinoma), MCF-7 (breast carcinoma), and MDA-MB-436 (breast carcinoma). However, the cytotoxicity toward noncancerous cells having typical membrane compositions, such as HUVEC and erythrocytes, is low. CD spectroscopy, appropriately designed peptide controls, cell-based studies, liposome leakage assays, and electron microscopy support the intended mechanism of action, which leads to preferential killing of cancerous cells.

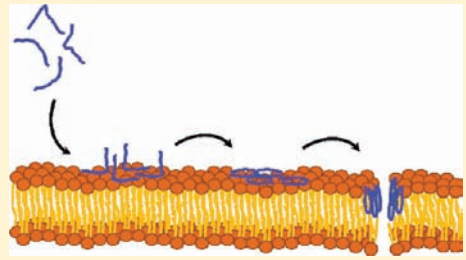

INTRODUCTION

Normal mammalian cell membranes are characterized by an asymmetric distribution of phospholipid type between the two leaflets of the lipid bilayer. The outer leaflet contains mostly zwitterionic lipids, such as phosphatidylcholine and sphingomyelin, displaying an overall neutral charge. The inner leaflet contains mainly phosphatidylethanolamine and phosphatidylserine (PS), resulting in an overall net negative charge.[1,2] Loss of lipid asymmetry, due to the translocation of PS to the outer leaflet, is found to occur in several biological and pathological processes.[3−6] The transbilayer movement of PS is mediated by several enzymes including aminophospholipid translocase and scramblase, which are responsible for the maintenance and collapse, respectively, of bilayer asymmetry.[6−10] Importantly, cell-surface exposure of PS occurs in a number of tumor cells[11,12] and endothelial cells comprising tumor blood vessels,[13,14] allowing this surface presentation to be used as a marker or target in cancer therapy.[11,14−16] In addition to the loss of PS asymmetry, changes in the glycosylation pattern of glycoproteins on the surface of cancer cells results in a high level of sialic acid on aberrant O-glycosylated mucins.[17−19] The presence of anionic PS, along with changes in protein glycosylation contributes to a higher net negative charge on the surface of cancer cells when compared to that of normal cells.

Several cationic antimicrobial peptides (AMPs) have been found to show anticancer activity.[20−25] AMPs are cationic, amphiphilic molecules with opposing hydrophobic and polycationic faces. Their mechanism of action usually entails the disruption of cancer cell membranes, which are similar to bacterial cell membranes with respect to their electronegative character. The cationic face of an AMP is responsible for engaging the electronegative surface of the cancer cell via hydrogen bonding and electrostatic interactions. Once bound to the outer leaflet of the membrane, the hydrophobic face of the AMP facilitates peptide insertion into the lipid portion of the bilayer. This ultimately disrupts the structural integrity of the membrane, which leads to cell death.

Most AMPs that are active against cancer cells are unstructured in aqueous solution but adopt a bioactive, helical conformation at the cell surface. Folding is driven by the formation of favorable interactions between the membrane surface and the amphiphilic peptide.[20−25] Although the

Received: November 10, 2011
Published: March 13, 2012

bioactive conformation of most anticancer AMPs is helical, there are a few that adopt β-structure. However, unlike helical AMPs that adopt their bioactive conformation at the cell surface, these β-rich AMPs are folded prior to engaging the membrane. To accomplish this, these peptides use extensive conformational constraints, typically disulfide bonds, to stabilize their bioactive conformation.[20−24]

Anticancer peptides that are unstructured in solution, but that adopt bioactive β-structure at the surface of cells to elicit their action are not known. Herein, we report the design of a small anticancer peptide that folds at the surface of cancer cells, adopting an amphiphilic β-hairpin structure capable of membrane disruption (Figure 1A). The 18-residue peptide

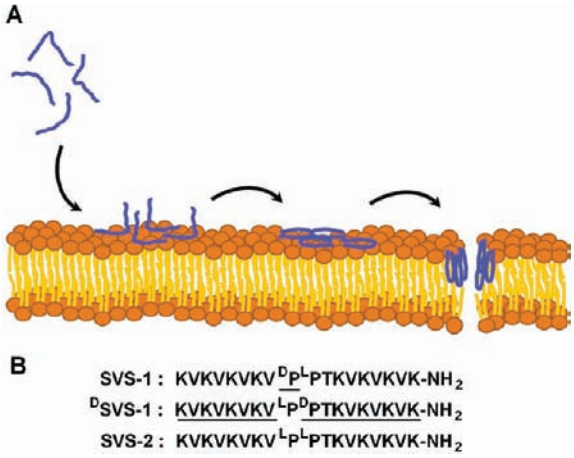

Figure 1. Membrane-induced folding and subsequent interpolation of β-hairpin anticancer peptide (SVS-1). (A) SVS-1 exists in a random coil conformation in solution. On engaging the negatively charged membrane surface, SVS-1 folds into a bioactive, lytic β-hairpin conformation capable of membrane disruption. (B) Peptide sequences of SVS-1 and its controls. Underlined amino acids are D-isomers, and all others are L-isomers; the stereochemistry of turn region is specified for clarity.

was designed to be unfolded in aqueous solution. However, in the presence of negatively charged membrane surfaces, the cationic peptide engages the membrane through electrostatic interactions, and folds at the surface adopting an amphiphilic structure capable of membrane disruption. Thus, no conformational constraints are needed to realize the bioactive conformation, and the peptide's lytic activity is turned on at the surface of cells that are highly electronegative in character, providing a means of enabling preferential action.

EXPERIMENTAL SECTION

Materials. Fmoc-protected amino acids were purchased from Novabiochem. PL-Rink resin was purchased from Polymer Laboratories. 1*H*-Benzotriazolium 1-[bis(dimethylamino) methylene]-5chloro-hexafluorophosphate (1-),3-oxide (HCTU) was obtained from Peptides International. Trifluoroacetic acid was obtained from Acros organics. 1,2-ethanedithiol and ethylenediaminetetraacetic acid (EDTA) was purchased from Fluka. Diethyl ether and sodium fluoride (NaF) were purchased from Fisher Scientific. Thioanisole, anisole, 3-(4,5-dimethyl-2-thiazolyl)-2,5-diphenyl-2*H*-tetrazolium bromide (MTT), dimethyl sulfoxide (DMSO), 200 mM glutamine solution, triton X-100, (CF), and bis-tris-propane (BTP), terbium(III) chloride hexahydrate ($TbCl_3 \cdot 6H_2O$), 2,6-pyridinedicarboxylic acid (dipicolinic acid, DPA), octyl β-D-glucopyranoside (OG), sodium citrate and *N*-[Tris(hydroxymethyl) methyl]-2-aminoethanesulfonic acid (TES) were obtained from Sigma-Aldrich. RPMI-1640 media was purchased from Invitrogen. EGM-2 media was purchased from Lonza. Heat-inactivated fetal bovine serum (FBS), penicillin and streptomycin solution, and trypsin EDTA were obtained from Hyclone Laboratory Inc. Cytotoxicity detection kit (LDH) was obtained from Roche Applied Science. 1-Palmitoyl-2-oleoyl-*sn*-glycero-3-phosphocholine (POPC) and 1-palmitoyl-2-oleoyl-*sn*-glycero-3-phospho-L-serine (POPS) were purchased from Avanti Polar Lipids. SephadexTM G-50 medium was purchased from GE Healthcare Biosciences.

Peptide Synthesis and Purification. Peptides were synthesized on PL-Rink resin using an automated ABI 433A peptide synthesizer. Synthesis was carried out via Fmoc-based solid-phase peptide chemistry with HCTU activation. Dried resin-bound peptides were cleaved from the resin and simultaneously side-chain deprotected using a trifluoroacetic acid/thioanisole/1,2-ethanedithiol/anisole (90:5:3:2) cocktail for 2 h under argon atmosphere. Crude peptides were precipitated with cold diethyl ether and then lyophilized. Reverse-phase HPLC equipped with a semi-preparative Vydac C18 column was employed to purify the peptides. HPLC solvents consisted of solvent A (0.1% TFA in water) and solvent B (0.1% TFA in 9:1 acetonitrile/water). Linear gradients consisted of 14−100% solvent B over 172 min for SVS-1, 13−100% over 174 min for DSVS-1, and 11−100% over 178 min for SVS-2. Peptide solutions were collected and then lyophilized. The purity of peptides was verified by analytical HPLC and electrospray ionization (ESI-positive mode) mass spectrometry. Analytical HPLC chromatograms and ESI (+) mass spectra for the pure peptides are shown in the Supporting Information.

Cell Culture. Adherent cancer cell lines (A549, lung carcinoma; KB, epidermal carcinoma; MCF-7, breast carcinoma; and MDA-MB-436, breast carcinoma) obtained from ATCC were each cultured as a monolayer in growth media containing RPMI-1640 media, 10% heat-inactivated fetal bovine serum (FBS), 2 mM glutamine, 100 U/mL penicillin and 100 U/mL streptomycin. Human umbilical vein endothelial cells (HUVEC) purchased from Lonza were cultured as a monolayer in EGM-2 media. All cell cultures were maintained at 37 °C and 5% CO_2 in a humidified environment.

Peptide Solution Preparation. Lyophilized peptides were first dissolved in filtered, deionized water. For cell-related studies, a 2 mM peptide solution was diluted to desired concentrations in either serum-free RPMI-1640 growth media for cancer cell lines or 2% FBS-containing EGM-2 media for HUVEC. For the hemolysis study, an equal volume of ice-cold peptide stock solution in filtered, deionized water was mixed with ice-cold pH 7.4 TN buffer (20 mM Tris, 300 mM NaCl). The final concentrations of peptide are 0.1, 1, 10, 100, 200, 500, and 1000 μM in 10 mM Tris buffer pH 7.4 with 150 mM NaCl.

Cell Proliferation Assay. A MTT assay was employed to assess the in vitro cytotoxicity of the peptides. A549, KB, and HUVEC cells were seeded onto a 96-well plate at 5000 cells/100 μL/well and incubated for 24 h. MCF-7 and MDA-MB-436 cells were seeded at 10,000 cells/200 μL/well and incubated for 48 h. All cells were plated in quadruplicate. After the media was removed, 100 μL of the peptide solution (prepared as described above) ranging from 0.01 to 100 μM was added to the wells. Serum-free RPMI-1640 growth media or 2% FBS-containing EGM-2 media was used as a control for 100% viability (untreated cells). Twenty percent DMSO-containing media was used as a negative control. Following 24 h incubation, a 10 μL solution of freshly prepared 5 mg/mL MTT in PBS was added to each well and allowed to incubate for an additional 2 h for cancer cell lines or 4 h for HUVEC cells. Then, the media/peptide/MTT solution was removed, and spectrophotometric grade DMSO was added at 150 μL/well. Plates were then shaken on an orbital shaker to facilitate formazan crystal solubilization. The absorbance was measured at 540 nm using a microplate reader (Biotek, Winooski, VT). The percent viability was calculated as follows: $(\text{Absorbance}_{\text{peptide-treated cells}}/\text{Absorbance}_{\text{untreated cells}}) \times 100$, and the percent cell death was calculated as follows: 100 − (percent viability). IC_{50}values were computed by Graphpad 5.0 software package and are shown as an average of at least three independent experiments.

Lactate Dehydrogenase (LDH) Assay. In order to monitor membrane leakage, an LDH assay was performed according to the

manufacturer's instructions. Briefly, A549 cells were plated into a 96-well plate in quadruplicate as described above and allowed to incubate for 24 h. The media was subsequently removed, and cells were incubated with various concentrations of peptide at 200 μL/well for 24 h. Serum-free RPMI-1640 growth media was used as a control for background LDH release, and 2% triton X-100 in serum-free media was used as a control for maximal LDH release. To measure LDH release, 100 μL/well of assay media was transferred from the cell culture plate into a new 96-well plate, followed by the addition of 100 μL of freshly prepared LDH assay solution into each well. The plates were incubated for 30 min at room temperature. Then, the absorbance was measured at 490 nm using a microplate reader (BioteK, Winooski, VT). Percent LDH release was calculated using the following equation: $((\text{Absorbance}_{\text{peptide-treated cells}} - \text{Absorbance}_{\text{untreated cells}})/(\text{Absorbance}_{\text{triton-X100 treated cells}} - \text{Absorbance}_{\text{untreated cells}})) \times 100$. Dose response curves shown are an average of three independent experiments.

Hemolysis Assay. Fresh human blood samples were obtained from the Research Donor Program at the National Cancer Institute (Frederick, MD) on the day of the experiment. The blood was washed three times with pH 7.4 TN buffer (10 mM Tris, 150 mM NaCl) and centrifuged at 3460 rpm for 10 min at 4 °C to retrieve human red blood cells (hRBCs). In a 96-well polypropylene plate, 100 μL of a 2× peptide solution in TN buffer (prepared as described above) was added to the wells and then mixed with 100 μL of 0.25% v/v hRBCs in TN buffer. The 0% hemolysis and 100% hemolysis controls consisted of hRBCs treated with TN buffer and 1% Triton X-100 in TN buffer, respectively. For the assay, the plates were incubated for either 1 or 24 h at 37 °C on an orbital shaker with slow agitation. The solution was then centrifuged at 14000 rpm for 10 min at 4 °C, and the supernatant was transferred into a new 96-well polystyrene plate. Absorbance was measured at 415 nm using a microplate reader (Biotek, Winooski, VT), and percent hemolysis was calculated using the following equation: $((\text{Absorbance}_{\text{treated hRBC}} - \text{Absorbance}_{\text{untreated hRBC}})/(\text{Absorbance}_{\text{triton-X100 treated hRBC}} - \text{Absorbance}_{\text{untreated hRBC}})) \times 100$. Each experiment was performed in triplicate, and the dose response curve is an average from two independent blood donors.

Circular Dichroism Spectroscopy. Circular dichroism (CD) experiments were performed to determine the secondary structure of the peptides in aqueous buffer solution and in the presence of model lipid membranes. Large unilamellar vesicles (LUV) were used as a model membrane system for the CD studies. LUV of POPC and POPC/POPS (1:1) were prepared by extrusion techniques. Briefly, POPC or POPC and POPS solutions in chloroform were dried under a gentle stream of argon. Solvent removal was completed in vacuum for 16 h. The lipid film was hydrated in a pH 7.4 buffer (50 mM BTP, 150 mM NaF) and subjected to eight freeze–thaw cycles. Then, the lipid solutions were extruded using 100-nm pore size filters to obtain LUV. CD spectra of the peptides were obtained in aqueous solution (50 mM BTP, 150 mM NaF, pH 7.4) and in the presence of LUV (final lipid concentration 2.5 mM). Peptide solutions (50 μM) were used to give a peptide/lipid ratio of 1:50. Wavelength spectra were measured from 200 to 260 nm at 37 °C using a 0.1 mm path length quartz cell. The mean residue ellipticity, $[\theta]$, was calculated from the equation $[\theta] = (\theta_{\text{obs}}/10lc)/r$, where θ_{obs} is the measured ellipticity (mdeg), l is the length of the cell (cm), c is the molar concentration, and r is the number of residues. CD spectra were collected on an AVIV model 420 circular dichroism spectrometer (AVIV Biomedical, Lakewood, NJ).

Electron Microscopy. A549 or HUVEC cells were seeded at 150,000 cells/3 mL/well onto coverslips that are placed into a 6-well plate for scanning electron microscopy (SEM) analysis. The same cell concentration of A549 was also plated onto a 6-well plate for transmission electron microscopy (TEM) analysis. The plates were allowed to incubate overnight at 37 °C and 5% CO_2 in a humidified atmosphere. After removing the media, 8 μM of SVS-1 in serum-free RPMI-1640 growth media was added to each well for A549 cells and 80 μM of SVS-1 in EGM-2 media was added to each well for HUVEC cells. The plates were incubated for 4 h under the same conditions. Then, the peptide solution was removed, and cells were briefly rinsed with 1 mL of PBS. After removing the PBS, 5 mL of warm fixative solution (2% gluteraldehyde in 0.1 M cacodylate buffer, pH 7.2) was added. The plates were incubated at room temperature for 1 h and then stored at 4–8 °C until imaged.

For TEM, the cells were post fixed in 1% w/v osmium tetroxide in 0.1 M cacodylate buffer, pH 7.2, for 1 h and *en bloc* stained with 0.5% uranyl acetate in 0.1 M acetate buffer, pH 4.2. The cells were subsequently dehydrated in graded ethanol solutions (35%, 50%, 70%, 95%, and 100%) and infiltrated overnight in epoxy resin (Poly/Bed 812, Polysciences). After changing the embedding medium with fresh pure resin, the plates were cured for 48 h at 55 °C. When the polystyrene plates were removed, suitable areas for thin sectioning were selected, cut out with a jewelry saw, and glued onto empty resin stubs. Approximately 70-nm-thin sections were cut on an ultramicrotome (Leica UC 6) and mounted on naked copper grids. The thin sections were double stained (uranyl acetate and lead citrate) and examined in a Hitachi H-7600 transmission electron microscope; the images were created using an AMT CCD camera.

For SEM, the cells were postfixed with 1% w/v osmium tetroxide in 0.1 M cacodylate buffer, pH 7.2 for 1 h and then dehydrated in an ascending ethanol series (35%, 50%, 70%, 95%, and 100%). The samples were transferred to fresh tetramethylsilane (TMS), incubated three times for 10 min each, and then air-dried. Samples were mounted on metal stubs using double-sided sticky tape and were sputter coated with about 5 nm of gold/palladium before SEM observations were performed in a Hitachi S-3000N scanning microscope.

Liposomal Tb/DPA Leakage Assay. Liposomes of desired formulation (either 1:1 POPC/POPS or pure POPC) were prepared by probe sonication. Specifically, POPC and POPS were dissolved separately in chloroform and mixed at desired molar ratios. A lipid film was formed by removing the chloroform via a stream of nitrogen at room temperature. Any residual chloroform was removed by placing the films overnight in a vacuum desiccator. Multilamellar liposomes containing the fluorescent Tb/DPA complex were formed by reconstituting lipid films with the following solution: 7.5 mM $TbCl_3$, 75 mM sodium citrate, 75 mM sodium dipicolinate, 10 mM TES, pH 7.4 by vigorous vortexing. Multilamellar liposomes were sonicated at 4 °C by using a Probe Sonicator (Branson Ultrasonics (Shanghai) Co., Ltd., China). Usually, 10 min of sonication (1-min pulses and 1-min rest) yielded unilamellar liposomes in the size range of ~100 nm in diameter, as determined by dynamic light scattering using a Zeta Nanosizer. The resulting unilammelar lioposomes were centrifuged at 1500 × g for 5–10 min to remove any titanium particles from the sonication probe and large lipid aggregates. Tb/DPA-loaded liposomes were purified further by size-exclusion gel chromatography to remove free Tb/DPA (Sephadex G-50, pre-equilibrated with 100 mM NaCl, 10 mM TES, 1 mM EDTA, at pH 7.4). Column fractions were analyzed by fluorescence. Liposome fractions containing Tb/DPA were pooled, and the total phospholipid concentration was determined by inorganic phosphate analysis.[26]

The Tb/DPA leakage assay from liposomes was performed using a fluorimeter (Fluoromax-3, Horiba Jobin Yvon, United States) and a quartz cuvette under constant stirring. Tb/DPA-containing liposomes in buffer (100 mM NaCl, 10 mM TES, 1 mM EDTA, at pH 7.4) were diluted by the addition of 10 mM TES, 100 mM NaCl, pH 7.4 to achieve a final lipid concentration of 25 μM and a concurrent EDTA concentration of 0.1 mM for the assay. The luminescence of liposomes containing terbium/DPA (excitation at 278 nm, emission at 545 nm) was measured as a function of time and added peptide (1 μM final concentration). Specifically, a cuvette containing a solution of liposomes was introduced to the fluorimeter, and the luminescence intensity was allowed to equilibrate (several minutes). Then, peptide was added resulting in a peptide/lipid ratio of 1:25, and the decrease in intensity was measured. After equilibration, octyl β-D-glucopyranoside (OG) was added (1% w/v final concentration) to induce 100% leakage. Leakage of liposome content (e.g., encapsulated Tb/DPA) results in a decrease in luminescence intensity due to the complexation of Tb^{3+} ion by EDTA present in the external buffer. Luminescence intensity in the absence of peptide represents 0% leakage, and the

luminescence intensity after the addition of OG represents 100% leakage. The extent of release as a function of time, $R(t)$, may be calculated from $R(t) = 100 \times [I(0) - I(t)]/[I(0) - I(f)]$, where $I(t)$ is the luminescence intensity at time t, $I(0)$ is the initial luminescence of the Tb/DPA liposomes before any peptides are added, and $I(f)$ is the luminescence obtained after the addition of OG.[27]

RESULTS AND DISCUSSION

Peptide Design. SVS-1 is an 18-residue peptide designed to fold into a bioactive, β-hairpin conformation at the surface of negatively charged membranes, Figure 1. The peptide contains N- and C-terminal strand regions of alternating valine (Val) and lysine (Lys) residues connected by an intermittent tetrapeptide (−V^{D}PPT−). The tetrapeptide is a consensus sequence designed to adopt a type II′β-turn.[28] In solution at neutral pH, SVS-1 should adopt an ensemble of random coil conformations where the turn region of the peptide is structured, but the appended strand regions are largely unstructured, Figure 1. In the absence of any compensatory interactions, the high density of positive charge from the lysine side chains, results in intrastrand charge repulsion, keeping the N- and C-terminal strands from interacting to form the folded β-hairpin. However, when SVS-1 contacts the electronegative surface of the cell membrane, the lysine-borne positive charge should be pacified as ion pairs are formed, allowing the terminal strands to collapse to form the folded amphiphilic hairpin. This surface-induced folding event is made possible via the delicate thermodynamic balance of biophysical forces that oppose and favor folding. For SVS-1, the electrostatic strand repulsion that opposes folding should be mitigated by the formation of favorable ion pairs between the membrane surface and the peptide, as well as the formation of intramolecular H-bonds that define the sheet portion of the hairpin. The alternating placement of Val and Lys residues ensures that in the folded state, SVS-1 displays one lysine-rich face, which engages the surface of outer leaflet, and an opposing hydrophobic face composed of valine side chains. Because solvation of the valine-rich face by water is energetically unfavorable, folded SVS-1 should interpolate into the lipid portion of the bilayer.

Additional, more subtle, design features were also incorporated into SVS-1. Amphiphilic peptides tend to self-associate when dissolved in aqueous solution. From our work in designing β-sheet self-assembling peptides,[29−31] we have found that the incorporation of hydrophobic residues at the N- and C-termini of peptides favors self-assembly, but incorporating charged residues at these positions strongly disfavors assembly.[32] The molecular basis of this observation is not yet known, but is under study in our lab. One can also tune a peptide's propensity to self-assemble by varying the number of hydrophobic residues relative to hydrophilic residues. Thus, in order to prevent the self-association of SVS-1 in solution prior to its engagement of the cell membrane, Lys residues were placed at its N- and C-termini, and the ratio of Lys to Val residues was kept at 8:6. As will be shown, only when the peptide encounters a negatively charged surface, such as a cancer cell membrane, does the charge on the Lys face become screened, promoting folding and subsequent burial of the hydrophobic face into the lipid bilayer.

Control peptides were also designed to confirm that the proposed mechanism of action of SVS-1 was membrane-induced β-hairpin folding and subsequent membrane disruption, Figure 1B. An all D-isomer of the peptide (^{D}SVS-1) was used to confirm that the mechanism of observed anticancer activity was membrane lysis and not receptor-mediated. An additional control peptide (SVS-2) was prepared to determine if SVS-1 truly needs to adopt a β-hairpin structure to be active. The sequence of SVS-2 is nearly identical to that of SVS-1 with the exception of one residue at position 10. Here, the ^{D}Pro of SVS-1 is replaced with ^{L}Pro. This small stereochemical change disrupts β-turn formation and forces the peptide to adopt an extended, linear conformation.[33] Thus, if β-hairpin folding is necessary for activity, then SVS-2 should be inactive.

Cytotoxic Activity. The in vitro activity of the SVS-1 peptide was studied using four different cancer cell lines: A549 (lung carcinoma), KB (epidermal carcinoma), MCF-7 (breast carcinoma) and MDA-MB-436 (breast carcinoma). Figure 2

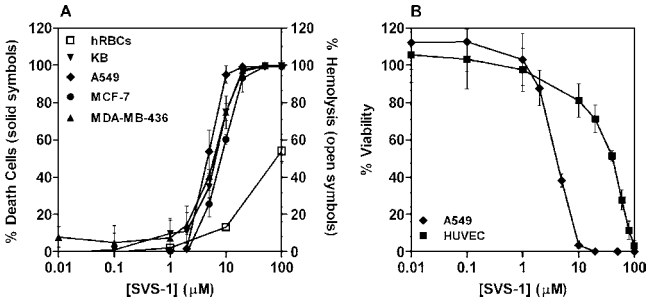

Figure 2. (A) In vitro cytotoxicity of SVS-1 toward A549 lung carcinoma, KB epidermal carcinoma, MCF-7 breast adenocarcinoma, MDA-MB-436 breast adenocarcinoma, and human erythrocytes (hRBCs); (B) cytotoxicity toward A549 and human umbilical vein endothelial cells (HUVEC). The cytotoxicity of SVS-1 was assessed at 24 h post addition of peptide. Error bars represent standard deviation of at least three independent experiments for the MTT assays used to measure % cell death, and of two independent blood donors for the hemolysis assay.

shows an MTT assay where the cells were exposed to increasing concentrations of SVS-1 for 24 h. The data clearly show that the peptide's cytotoxic activity is dose-dependent against all the cancer cell lines tested, with IC_{50} values that range from 4.9 ± 0.6 to 8.1 ± 0.8 μM (Table 1). The IC_{50} values obtained for SVS-1 are comparable to other anticancer β-hairpin AMPs. For example, the IC_{50} of lactoferricin B is in the range of 15.5−60 μM,[34] while the IC_{50} of gomesin is about 1.4−8.1 μM.[35]

The selectivity of SVS-1 was first investigated using human red blood cells (hRBCs). hRBCs are easily procured, and their simple, neutral membranes make them an excellent system to probe the folding-dependent activity of SVS-1.[2] The lytic activity of SVS-1 toward human hRBCs is also shown in Figure 2 by coplotting the percent hemolysis as a function of peptide concentration after 24 h incubation at 37 °C. The data show that SVS-1 is preferential in its action, having an HC_{50} value of 80.8 ± 12.8 μM. In the literature, hemolytic activity is often determined from experiments having short incubation times, typically 1 h. For comparison, we also investigated the hemolytic activity of SVS-1 using a 1 h incubation time. In this experiment, the hemolytic activity of 100 μM peptide is about 16.3 ± 6.0% (n = 4), and the HC_{50} value was determined to be greater than 1 mM (Table 1). This level of hemolysis is relatively low when compared to other lytic, anticancer peptides. For example, at 100 μM, gomesin showed 35−40% hemolysis,[36] whereas tachyplesin I displays 30−100% hemolysis after 1 h incubation.[37,38] The 24 h IC_{50} and HC_{50} data were used to calculate the therapeutic index (TI) for SVS-1 with

dx.doi.org/10.1021/ja210569f | J. Am. Chem. Soc. 2012, 134, 6210−6217

Table 1. Cytotoxicity of Peptides toward Cancer Cell Lines and Human Erythrocytes (hRBCs)

	IC_{50} (μM)[a]						therapeutic index[c]			
peptide	A549	KB	MCF-7	MDA-MB-436	$HC_{50-1\ h}$[b] (μM)	$HC_{50-24\ h}$[b] (μM)	A549	KB	MCF-7	MDA-MB-436
SVS-1	4.9 ± 0.6	6.3 ± 0.7	8.1 ± 0.8	5.6 ± 0.5	>1000	80.8 ± 12.8	16.7	12.9	10.0	14.5
^{D}SVS-1	3.2 ± 0.6	4.5 ± 0.5	4.7 ± 0.4	3.2 ± 0.4	>1000	n.d.[d]	–	–	–	–
SVS-2	>100	>100	>100	>100	>1000	n.d.[d]	–	–	–	–

[a]Inhibitory concentration resulting in 50% cell death compared to untreated cells. [b]Concentration at which 50% hemolysis was observed after either 1 or 24 h post-incubation with the peptides. [c]Peptide cytotoxicity toward indicated cell types relative to hRBCs ($HC_{50-24\ h}/IC_{50\ indicated\ cells}$). [d]n.d.: not determined.

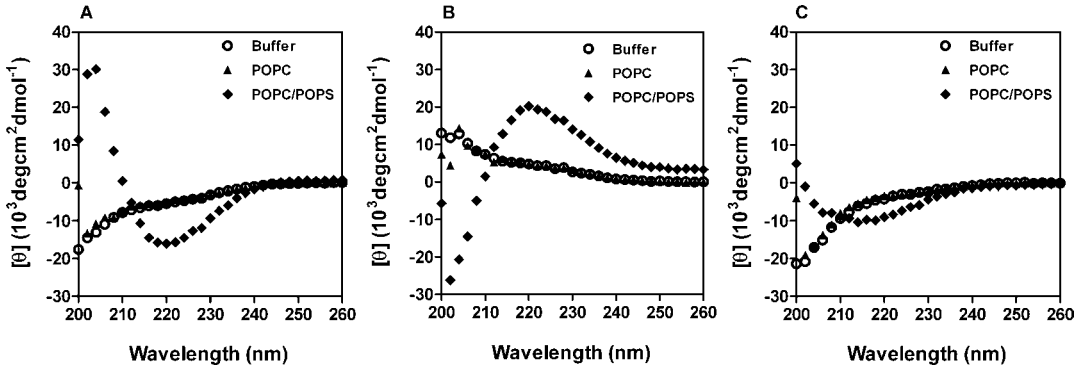

Figure 3. CD spectra of 50 μM (A) SVS-1 (B) ^{D}SVS-1, and (C) SVS-2 in the following: (○) aqueous buffer solution (50 mM BTP, 150 mM NaF, pH 7.4), (▲) in the presence of neutral POPC LUVs, and (♦) in the presence of negatively charged POPC/POPS LUVs (1:1).

respect to the different cancer cell lines and can serve as a qualitative measure of membrane preference. TI ratios range from 10 to 17, showing that the peptide is considerably less toxic to normal cells when compared to cancer cells.

The anticancer activity of the enantiomeric control peptide, ^{D}SVS-1, was also investigated. Table 1 shows that ^{D}SVS-1displays levels of toxic activity against the cancer cells similar to those of its mirror image peptide, with IC_{50} values in the range of 3−5 μM. This suggests that SVS-1 acts via a lytic mechanism and not a mechanism involving specific receptor binding. The second control peptide, SVS-2, was also examined against the four cancer cell lines and hRBCs. SVS-2 was designed to adopt an extended, linear conformation and to test the hypothesis that hairpin formation is necessary for SVS-1 activity. The IC_{50} and HC_{50} values are shown in Table 1 and indicate that this control peptide shows negligible toxicity toward both cancer cell lines and hRBCs at the maximum concentrations tested (100 μM for cancer cells and 1 mM for hRBCs).

An additional experiment was performed to further investigate the selectivity of SVS-1's lytic action using primary human umbilical vein endothelial cells (HUVEC). Figure 2B shows percent viability of HUVEC and A549 cells when exposed to increasing concentrations of SVS-1 for 24 h. The IC_{50} value for SVS-1 toward HUVEC is 36.1 ± 4.0 μM, which is 7-fold higher than that obtained for the A549 cells.

Membrane-Induced Folding of SVS-1. The cell-based studies suggest that SVS-1 acts through a lytic mechanism that entails β-hairpin folding at the membrane surface. Circular dichroism (CD) spectroscopy was used to investigate this assertion by monitoring the secondary structure of SVS-1 in the presence and absence of model membranes, Figure 3A. The CD spectrum of an aqueous solution of SVS-1 alone (50 μM peptide, 50 mM BTP, 150 mM NaF, pH 7.4) at 37 °C is indicative of random coil conformation. Also shown is the spectrum of SVS-1 in the presence of neutral lipid vesicles made of POPC, which indicates that peptide is again unfolded. Both these spectra demonstrate that SVS-1 is incapable of folding in solution or at the surface of a purely neutral membrane. However, when SVS-1 is added to a solution containing negatively charged lipid vesicles, made from a 1:1 mixture of POPC/POPS, the resulting CD spectrum shows a distinct minimum in mean residue ellipticity at 218 nm, indicating that the peptide adopts β-sheet structure consistent with hairpin formation, presumably at the surface of the negatively charged vesicles. Figure 3B shows the identical experiment for ^{D}SVS-1, the mirror image control peptide. As expected, the resulting spectra are the mirror images of those obtained for SVS-1 and show that ^{D}SVS-1 behaves in a similar fashion, folding only in the presence of negatively charged vesicles. Figure 3C shows the identical experiment for control peptide SVS-2, which is incapable of intramolecular folding into a hairpin conformation, due to the two central ^{L}Pro residues in its sequence. The spectra indicate that this peptide adopts a random coil in buffer and in the presence of neutral vesicles. However, in the presence of negatively charged vesicles, the peptide adopts a mixture of random coil and β-sheet structure as evidenced by the blue shift of the β-minimum and a decrease in the positive ellipticity at 200 nm as compared to the spectrum of SVS-1. Since SVS-2 is incapable of adopting a β-hairpin conformation, we ascribe the β-component of its spectrum to be a result of the formation of a small amount of β-sheet-rich oligomer, resulting from intermolecular self-assembly induced by the negatively charged lipid. These β-assemblies are most likely biologically inactive since SVS-2 was incapable of killing any of the cancer cell lines examined even at concentrations greater than 100 μM. Taken together, the CD data indicate that the lysine-borne positive charge of SVS-1 is sufficient to keep the peptide in the unfolded state in solution but is instrumental in forming attractive electrostatic inter-

dx.doi.org/10.1021/ja210569f | J. Am. Chem. Soc. 2012, 134, 6210−6217

actions with the surface of negatively charged membranes where β-hairpin folding is triggered.

Membrane Disruption by SVS-1. Both the cell-based experiments and CD data are consistent with a mechanism that involves cell surface-induced folding followed by membrane disruption. To further investigate the possibility that SVS-1 is capable of compromising membrane integrity, leakage experiments were performed using model liposomes. In this assay, a luminescent terbium−dipicolinic acid (Tb/DPA) complex is encapsulated in both neutral (POPC) and negatively charged (1:1 POPC/POPS) liposomes. Excitation of the dipicolinic ligand at 278 nm results in the sensitized emission of terbium at 545 nm. Thus, intact liposomes are highly luminescent. However, perturbation of membrane integrity resulting in the release of the Tb/DPA complex leads to a decrease in luminescence intensity. As the Tb/DPA complex is released from the liposome, EDTA present in the external buffer displaces the DPA and chelates Tb ion, making energy transfer between the DPA and Tb inefficient. Figure 4 shows the

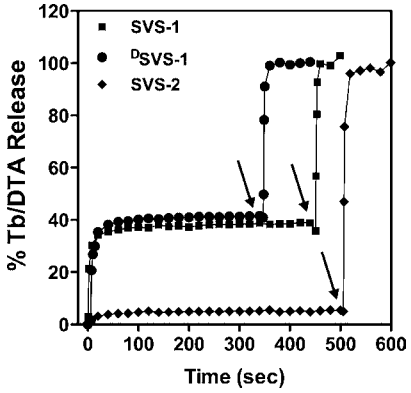

Figure 4. Tb/DPA release from model POPC/POPS (1:1) liposomes monitored as a function of time following the addition of peptide and subsequent detergent. Tb/DPA release was monitored via luminescence. At t = 0, peptides were added, and Tb/DPA release was measured as a function of time. Final peptide/lipid ratio was 1:25. After equilibrium was reached, 1% OG detergent was added to obtain 100% release (arrows).

percent Tb/DPA released as a function of time and added peptide. At t = 0, peptide is added and leakage monitored. The data show that when either SVS-1 or ^{D}SVS-1 is added to achieve a final peptide concentration of 1 μM (peptide/lipid ratio 1:25), leakage is induced from the negatively charged liposmes. This amount of peptide results in approximately 40% leakage. One hundred percent leakage is realized by the addition of detergent to the solution (indicated by the arrows). The rates at which both peptides induce leakage are similar and extremely fast. This suggests that both peptides act via similar mechanisms and that the most likely mechanism is nonspecific membrane disruption. The fast rate of induced leakage realized by SVS-1 in this assay is consistent with the fast killing action of this peptide as will be shown in the electron microscopy experiments discussed below. Conversely, leakage induced by the control peptide SVS-2 is minimal (<5%), suggesting that β-hairpin formation is required for activity. A similar experiment was performed with all three peptides using neutral liposomes prepared from POPC (Supporting Information). None of the peptides induced gross leakage (<5%) from these model neutral liposomes, indicating that a negatively charged surface is necessary to invoke the membrane-disturbing action of SVS-1 and ^{D}SVS-1. Taken together, the CD and liposome leakage experiments strongly suggest that SVS-1 folds at the surface of negatively charged membranes, adopting a conformation capable of membrane disruption.

To further investigate the mechanism of action in the context of cells, an in vitro assay was performed that measures the leakage of LDH, a cytoplasmic enzyme, from A549 cells that had been treated with SVS-1. Figure 5 shows the percent of

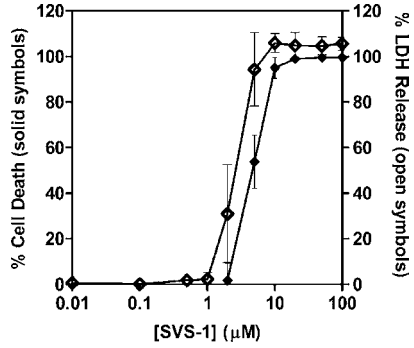

Figure 5. In vitro cytotoxicity of SVS-1 toward A549 cells and its effect on cell membrane leakage. % cell death was coplotted with % LDH release as a function of SVS-1 concentration. Error bars represent standard deviation of at least three independent experiments.

LDH released from the cells as a function of SVS-1 concentration, coplotted with percent cell death measured in a separate experiment. The plot nicely shows that as the concentration of SVS-1 increases, the amount of LDH released from the cells also increases and the number of dead cells increases. Importantly, the coplot derived from separate experiments shows that the concentration of peptide needed to induce 50% LDH leakage (~4 μM) is similar to the measured IC_{50} (4.9 ± 0.6 μM) of the peptide toward this cell line, Table 1, thus supporting a membrane disruption mechanism.

Lastly, electron microscopy studies (TEM and SEM) were performed to directly visualize cell membrane integrity as a function of added SVS-1. A549 cells were incubated with 8 μM (IC_{90}) SVS-1 for 4 h and imaged alongside untreated A549 cells. Representative TEM images of untreated and SVS-1-treated A549 cells are shown in Figure 6, A and D, respectively. Untreated cells have an intact cell membrane and clearly visible intact organelles. The cytoplasmic content is contained and appears light gray in the image. In contrast, cells that had been treated with SVS-1 show visibly disrupted membranes and leakage of both intraorganelle and cytoplasmic content as evident by the gray contrast. SEM micrographs B and E of Figure 6 are suggestive of a probable mode of action once SVS-1 is folded at the cell surface. Untreated A549 cells show smooth and intact cell membrane surfaces with regular cell morphology. On the other hand, SVS-1-treated cells appear to have sponge-like morphology, indicating that cell membrane disruption had occurred and that SVS-1 causes pore formation within the membranes it encounters. It is interesting to note that cells were fixed with glutaraldehyde in preparation for imaging after being treated with peptide for only 4 h. Thus, in agreement with the fast rate of membrane disruption observed in the liposomal leakage assays, cell membrane disruption also occurs quickly. Although the action of SVS-1 is preferential toward cancerous cells, it will kill noncancerous cells at higher

dx.doi.org/10.1021/ja210569f | J. Am. Chem. Soc. 2012, 134, 6210−6217

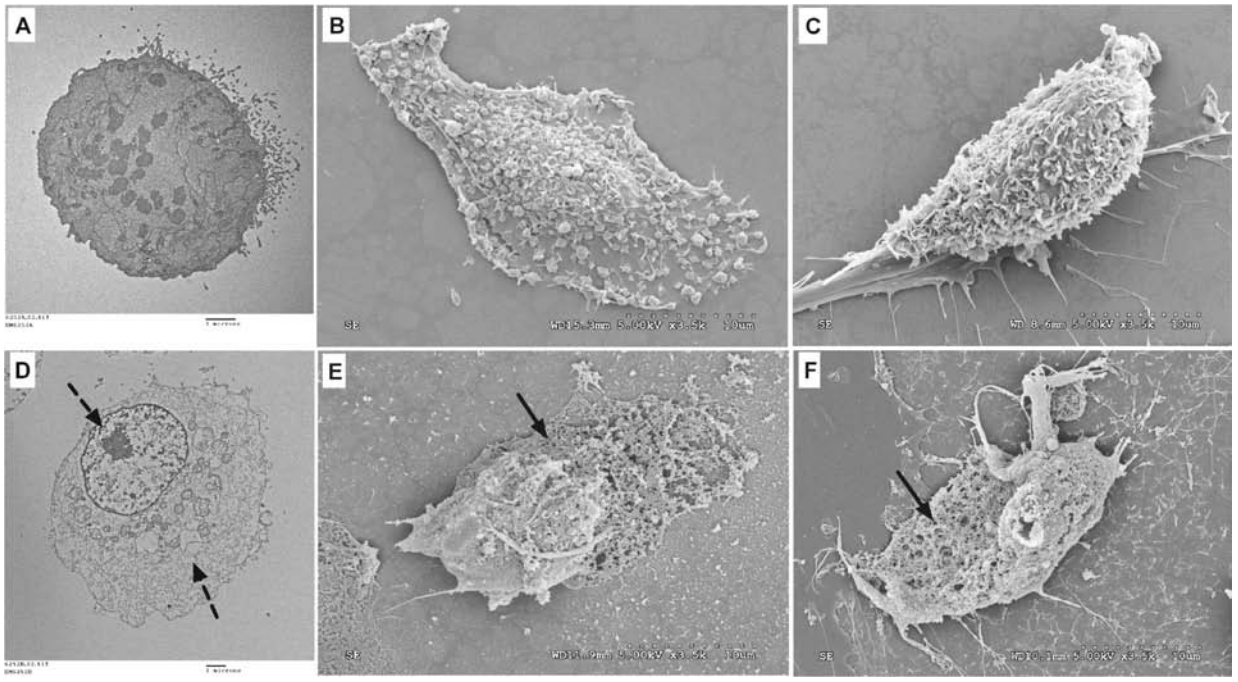

Figure 6. Effect of SVS-1 on cell membrane integrity observed by TEM (A,D) and SEM (C,B,E,F). Membranes of untreated A549 cancer cells (A,B) and noncancerous HUVEC (C) appeared intact. A549 cells (D,E) incubated with 8 μM SVS-1 in serum-free media. HUVEC cells (F) incubated with a large excess (80 μM) of SVS-1 for 4 h at 37 °C and 5% CO_2. Cells display leakage of cellular contents (dashed arrow) and pore formation (solid arrow). Scale bar: 10 μm for SEM, 2 μm for TEM.

concentration, Table 1. SEM was used to investigate the mode of action of a high concentration of SVS-1 toward noncancerous HUVEC cells. Figure 6C shows the healthy morphology of an untreated HUVEC cell, whereas Figure 6F shows the result of adding 80 μM SVS-1 to these cells. A nearly identical pattern of membrane disruption is observed, indicating that SVS-1 acts through a similar mechanism, irrespective of cell type.

An additional TEM experiment was performed to rule out a fibrillogenesis-based mechanism where SVS-1 forms fibrils after folding at the surface of negatively charged membranes and these fibrils are responsible for inducing membrane disruption. Samples of SVS-1 in the presence of negatively charged liposomes, obtained directly from CD experiments showing the formation of β-sheet structure, were imaged by TEM. Resulting micrographs (Supporting Information) showed only the presence of 100-nm-diameter liposomes and no peptide fibrils, making a fibrillogenesis-based mechanism unlikely. The spectroscopic, biophysical, microscopy, and cell-based data support an SVS-1 mechanism consistent with membrane-induced folding and consequent disruption via pore formation.

CONCLUSIONS

SVS-1 is an 18-residue peptide designed to fold at the surface of negatively charged cancer cell membranes, adopting an amphiphilic β-hairpin capable of disrupting membranes. To the best of our knowledge, this is the first example of an anticancer β-hairpin peptide whose action is dependent on membrane-induced folding. Since folding is requisite for function, SVS-1 is able to preferentially kill cancer cells, which contain a more electronegative cell surface as compared to noncancerous cells. SVS-1 shows low micromolar activity against A549 lung carcinoma, KB epidermal carcinoma, MCF-7, and MDA-MB-436 breast adenocarcinoma cell lines. The peptide exhibits low hemolytic activity toward hRBC and a moderate degree of selectivity when tested against HUVEC. Cell-based experiments, CD spectroscopy, liposomal leakage assays, and electron microscopy confirm a mechanism that entails cell membrane-induced folding of SVS-1 into an amphiphilic β-hairpin capable of interpolating and consequently disrupting the membranes of cancer cells via pore formation, ultimately resulting in cell death.

ASSOCIATED CONTENT

Supporting Information

Analytical HPLC chromatograms, ESI (+) mass spectra for the pure peptides, liposomal leakage assays, and TEM of SVS-1 in the presence of POPC:POPS liposomes. This materials is available free of charge via the Internet at http://pubs.acs.org.

AUTHOR INFORMATION

Corresponding Author

Joel.Schneider@nih.gov

Author Contributions

[Δ]These authors contributed equally.

Notes

The authors declare no competing financial interest.

ACKNOWLEDGMENTS

We thank Adam Harned, Christina Burks, and Ulrich Baxa from the Electron Microscopy Laboratory (SAIC-Frederick) for electron microscopy images and Marco Domingues for assistance with preliminary leakage experiments. This work was partially supported by a graduate fellowship awarded to C.S. through the Strategic Scholarship for Frontier Research Network (SFR) from the Office of the Higher Education Commission, Ministry of Education, Thailand. A Marie Curie International Outgoing Fellowship within the 7th European

Community Framework Programme partilly supported A.S.V. (PIOF-GA-2009-235154). D.G. acknowledges Fundação para a Ciência e a Tecnologia (Ministério da Educação e Ciência, Portugal) for Fellowship SFRH/BPD/73500/2010. Research funding was provided by the Intramural Research Program of the National Cancer Institute, National Institutes of Health.

REFERENCES

(1) Verkleij, A. J.; Zwaal, R. F. A.; Roelofsen, B.; Comfurius, P.; Kastelijn, D.; van Deenen, L. L. M. *Biochim. Biophys. Acta, Biomembr.* **1973**, *323*, 178.
(2) Zachowski, A. *Biochem. J.* **1993**, *294*, 1.
(3) Balasubramanian, K.; Schroit, A. J. *Annu. Rev. Physiol.* **2003**, *65*, 701.
(4) Chaurio, R.; Janko, C.; Muñoz, L.; Frey, B.; Herrmann, M.; Gaipl, U. *Molecules* **2009**, *14*, 4892.
(5) Vance, J. E.; Steenbergen, R. *Prog. Lipid Res.* **2005**, *44*, 207.
(6) Zwaal, R. F. A.; Comfurius, P.; Bevers, E. M. *Cell. Mol. Life Sci.* **2005**, *62*, 971.
(7) Bevers, E. M.; Comfurius, P.; Dekkers, D. W. C.; Zwaal, R. F. A. *Biochim. Biophys. Acta, Mol. Cell Biol. Lipids* **1999**, *1439*, 317.
(8) Comfurius, P.; Senden, J. M. G.; Tilly, R. H. J.; Schroit, A. J.; Bevers, E. M.; Zwaal, R. F. A. *Biochim. Biophys. Acta, Biomembr.* **1990**, *1026*, 153.
(9) Zhou, Q.; Zhao, J.; Stout, J. G.; Luhm, R. A.; Wiedmer, T.; Sims, P. J. *J. Biol. Chem.* **1997**, *272*, 18240.
(10) Bratton, D. L.; Fadok, V. A.; Richter, D. A.; Kailey, J. M.; Guthrie, L. A.; Henson, P. M. *J. Biol. Chem.* **1997**, *272*, 26159.
(11) Riedl, S.; Rinner, B.; Asslaber, M.; Schaider, H.; Walzer, S.; Novak, A.; Lohner, K.; Zweytick, D. *Biochim. Biophys. Acta, Biomembr.* **2011**, *1808*, 2638.
(12) Utsugi, T.; Schroit, A. J.; Connor, J.; Bucana, C. D.; Fidler, I. J. *Cancer Res.* **1991**, *51*, 3062.
(13) Ran, S.; Downes, A.; Thorpe, P. E. *Cancer Res.* **2002**, *62*, 6132.
(14) Ran, S.; Thorpe, P. E. *Int. J. Radiat. Oncol. Biol. Phys.* **2002**, *54*, 1479.
(15) Ran, S.; He, J.; Huang, X.; Soares, M.; Scothorn, D.; Thorpe, P. E. *Clin. Cancer Res.* **2005**, *11*, 1551.
(16) Kenis, H.; Reutelingsperger, C. *Curr. Pharm. Des.* **2009**, *15*, 2719.
(17) Yoon, W.-H.; Park, H.-D.; Lim, K.; Hwang, B.-D. *Biochem. Biophys. Res. Commun.* **1996**, *222*, 694.
(18) Burdick, M. D.; Harris, A.; Reid, C. J.; Iwamura, T.; Hollingsworth, M. A. *J. Biol. Chem.* **1997**, *272*, 24198.
(19) Reis, C. A.; Osorio, H.; Silva, L.; Gomes, C.; David, L. *J. Clin. Pathol.* **2010**, *63*, 322.
(20) Leuschner, C.; Hansel, W. *Curr. Pharm. Des.* **2004**, *10*, 2299.
(21) Papo, N.; Shai, Y. *Cell. Mol. Life Sci.* **2005**, *62*, 784.
(22) Schweizer, F. *Eur. J. Pharmacol.* **2009**, *625*, 190.
(23) Hoskin, D. W.; Ramamoorthy, A. *Biochim. Biophys. Acta, Biomembr.* **2008**, *1778*, 357.
(24) Mader, J. S.; Hoskin, D. W. *Expert Opin. Invest. Drugs* **2006**, *15*, 933.
(25) Papo, N.; Shai, Y. *Biochemistry* **2003**, *42*, 9346.
(26) Ames, B. N.; Dubin, D. T. *J. Biol. Chem.* **1960**, *235*, 769.
(27) Düzgünes, N.; Faneca, H.; Lima, M. C. *Methods Mol. Biol.* **2010**, *606*, 209.
(28) Nair, C. M.; Vijayan, M.; Venkatachalapathi, Y. V.; Balaram, P. *J. Chem. Soc., Chem. Commun.* **1979**, 1183.
(29) Schneider, J. P.; Pochan, D. J.; Ozbas, B.; Rajagopal, K.; Pakstis, L.; Kretsinger, J. *J. Am. Chem. Soc.* **2002**, *124*, 15030.
(30) Nagarkar, R. P.; Hule, R. A.; Pochan, D. J.; Schneider, J. P. *Pept. Sci.* **2010**, *94*, 141.
(31) Rughani, R. V.; Salick, D. A.; Lamm, M. S.; Yucel, T.; Pochan, D. J.; Schneider, J. P. *Biomacromolecules* **2009**, *10*, 1295.
(32) Geisler, I. M.; Schneider, J. P. *Adv. Funct. Mater.* **2012**, *22*, 529.
(33) Lamm, M. S.; Rajagopal, K.; Schneider, J. P.; Pochan, D. J. *J. Am. Chem. Soc.* **2005**, *127*, 16692.
(34) Eliassen, L. T.; Berge, G.; Leknessund, A.; Wikman, M.; Lindin, I.; Løkke, C.; Ponthan, F.; Johnsen, J. I.; Sveinbjørnsson, B.; Kogner, P.; Flægstad, T.; Rekdal, Ø. *Int. J. Cancer* **2006**, *119*, 493.
(35) Rodrigues, E. G.; Dobroff, A. S.; Cavarsan, C. F.; Paschoalin, T.; Nimrichter, L.; Mortara, R. A.; Santos, E. L.; Fazio, M. A.; Miranda, A.; Daffre, S.; Travassos, L. R. *Neoplasia* **2008**, *10*, 61.
(36) Fázio, M. A.; Oliveira, V. X.; Bulet, P.; Miranda, M. T. M.; Daffre, S.; Miranda, A. *Pept. Sci.* **2006**, *84*, 205.
(37) Katsu, T.; Nakao, S.; Iwanaga, S. *Biol. Pharm. Bull.* **1993**, *16*, 178.
(38) Rao, A. G. *Arch. Biochem. Biophys.* **1999**, *361*, 127.